

Adjustable 4-Level Hybrid Converter for Symbol Power Tracking in 5G New Radio

Hieu Pham¹, Ratul Das¹, Casey Hardy¹, Don Kimball^{1,2}, Peter Asbeck¹ and Hanh-Phuc Le¹

¹Department of Electrical and Computer Engineering

University of California San Diego, CA, USA

m1pham@ucsd.edu, hanhphuc@ucsd.edu

²Qorvo Inc.

Richardson, TX, USA

dfkimball@ucsd.edu

Abstract—A new adjustable multilevel hybrid (AMH) converter architecture is proposed for the radio frequency (RF) amplifier supply modulators using symbol power tracking. The converter comprises a 4-level switched-capacitor stage and an inductive partial-power-processing stage that allows four output levels to dynamically change depending on symbol power and communication traffic patterns in 5G New Radio (NR). The converter prototype provides a wide range of output voltages from 12V to 50V from a 50V input while delivering the output current up to 1A. It achieves efficiency higher than 85% for a wide range of RF loads and can deliver a maximum RF power of 50W with 98.4% efficiency. When tested with a commercial class-AB PA, a power-added efficiency improvement of 3X is achieved at 11 dB backoff power. The converter prototype supports symbol power tracking for 5G NR with a fast level transition below 50ns that is well within the cyclic prefix time allocated to avoid intersymbol interference.

Index Terms—DC-DC Converter, Envelope tracking, Symbol power tracking

I. INTRODUCTION

In modern communication systems, envelope tracking (ET) is one of the viable methods to enhance transmitters' efficiency. A simple diagram of an ET system is illustrated in Figure 1. In envelope tracking, the supply voltage of the power amplifier (PA) is dynamically adjusted by an envelope modulator to track the envelope of the RF signal amplitude corresponding to the RF power it needs to transmit. This allows the PA to operate near saturation throughout all operating points to improve power efficiency [1]. Various circuits can be used for the envelope modulator to provide the modulated supply voltage for the PA, such as a Buck converter [2], [3], or a combination of a switching converter in parallel or in series with a linear regulator [4]–[7]. However, increased RF signal bandwidth in wide-band radio, such as 5G New Radio (NR), requires a wide-band envelope modulator with a high switching frequency and large regulation bandwidth. This complicates the switching converter's design, increases loss, and negates or even eliminates the efficiency benefits of envelope tracking. In another solution to increase transition speed proposed in [8], [9], a multilevel converter is used to create multiple discrete voltage levels. Then an output switch network can quickly connect the output to one of these levels. This technique offers better adaptability to wide-band RF systems handled by the output network without the need for a high bandwidth regulation loop or high switching frequency in the multilevel converter. However, there remain

significant challenges to taking full advantage of the technique. RF signals typically have high peak-to-average ratios (PAPR), where the time the PA works at peak power only accounts for a small portion of the whole operation period. This would make the higher voltage levels in the multilevel supply modulator under-utilized. Therefore, it is desirable to have a larger number of levels to improve supply modulation efficiency and signal quality, but this leads to more complexity and additional losses that would undermine original benefits. While the multilevel tracking supply modulator was first introduced as an alternative to the traditional envelope tracking converter using an inductive switching converter, it became a prevailing solution as the signal bandwidth increased beyond 100 MHz in 5G NR. At the same time, as the signal bandwidth continued to increase, average power tracking (APT) and symbol power tracking (SPT) are now considered more efficient and more practical than envelope tracking. As shown in [10], APT for 4G LTE only requires supply modulation to change levels in every subframe of 1ms with $4.7\mu\text{s}$ maximum transition time in the allotted cyclic prefix, while these numbers in SPT for 5G NR are the symbol time of $4.16\mu\text{s}$ and 290ns cyclic prefix which can be seen in Figure 2. Therefore, SPT is chosen as the target application for this work because compared with APT, it has a better trade-off between tracking speed for efficiency and transition requirement. Hence, in addition to increasing the number of levels, it is desirable for the supply modulator to achieve a fast transition time below 100ns and well within the cyclic prefix.

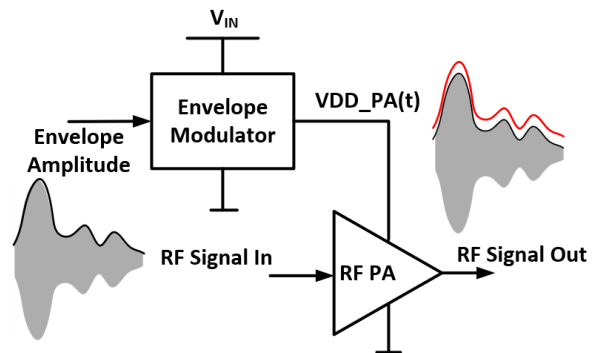


Fig. 1: Schematic diagram of PA with envelope tracking

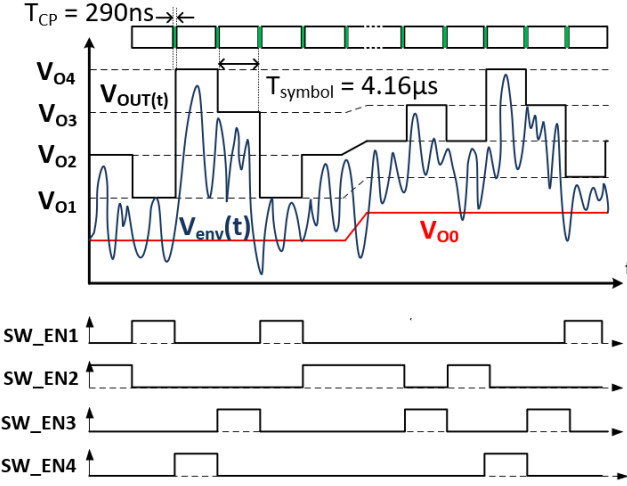


Fig. 2: Multilevel in SPT

In this paper, we propose a new adjustable multilevel hybrid (AMH) converter architecture for the envelope modulator, shown in Fig. 3. While having four primary levels from a multilevel switched-capacitor network, the proposed converter includes an inductive partial-power-processing stage with PWM control that allows the four levels to change dynamically to support a virtually infinite number of four level groups to cover a wide output voltage range up to the input voltage. The converter achieves efficiency higher than 85% for most of the RF load range, delivers up to 50W RF power with 98.4% peak efficiency, and supports a fast level transition within 50ns. The paper is organized as follows. Section II details the AMH converter architecture and operation. The proposed converter prototype implementation is presented in Section III. Section IV reports the performance of the converter, followed by the conclusion in Section V.

II. PROPOSED CONVERTER ARCHITECTURE

The proposed AMH converter architecture is shown in Fig. 3. The converter comprises three parts: a multilevel switched-capacitor (MLSC) converter stage based on the Ladder switched-capacitor (SC) topology, four output tracker switches, and a partial power processing (PPP) inductive stage to modulate the bottom level of the SC network. The MLSC stage comprises eight switches SW_{1-8} , three flying capacitors C_{F1-3} , and four output capacitors C_{O1-4} . The MLSC converter has 2 phases of operation, with the even switches SW_{2-8} turned ON in Phase Φ_1 and the odd switches SW_{1-7} turned ON in Phase Φ_2 to generate four voltage levels V_{O1-4} equally spaced between V_{O0} and V_{IN} (also V_{O4}). In other words, the three voltage levels at V_{O1-3} are $V_{Oi} = i \cdot \frac{V_{IN} - V_{O0}}{4} + V_{O0}$ where $i = [1; 3]$, or the voltage difference between two adjacent nodes of V_{Oi} is $\frac{V_{IN} - V_{O0}}{4}$. The ground level V_{O0} of the MLSC stage is generated by the PPP Buck-like inductive stage, using switches SW_B , diode D_{buck} and inductor L_{buck} . The input of the PPP stage is connected to V_{O1} node. Using simple PWM control, the PPP stage can

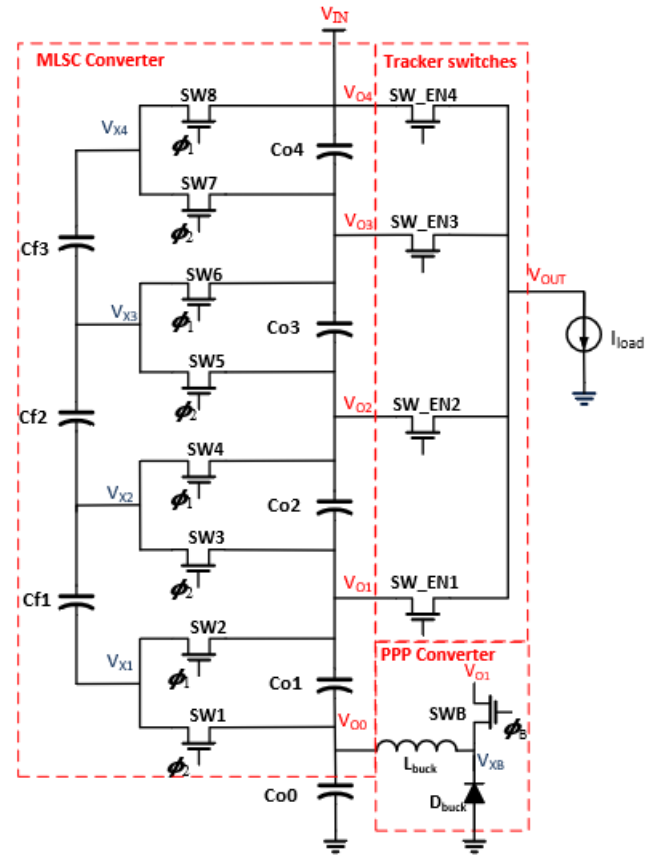


Fig. 3: AMH Converter architecture

redistribute the charge between C_{O1} and C_{O0} to regulate V_{O0} to different voltage levels. Hence, following the equal voltage distribution in the MLSC stage described above, the levels at V_{O1-3} are adjusted proportionally to generate different output voltages, as illustrated in Fig. 2. In this operation, the output power is partially processed by the MLSC converter and the PPP converter stages, while the PWM control in the PPP converter enables greater output regulation granularity, i.e. a virtually infinite number of output voltage levels, to improve output signal quality and overall system efficiency. Four tracker switches can be controlled separately to provide $V_{O1,2,3}$ and $V_{O4} = V_{IN}$ levels to the output V_{OUT} following a certain symbol voltage envelope to provide fast transitioning between the four output levels,

Note that the three stages of the converter can be optimized separately for their decoupled functions, MLSC and PPP stages for efficient average power delivery while the tracker stage for level transition and symbol rate tracking at 256kHz. As a result, while optimized differently, the switching frequency of the three converter stages and the regulation bandwidth of the PPP stage can be much smaller than the actual baseband RF signal, leading to reductions in switching loss and complexity of the control loop design.

TABLE I: Component list

| Component | Part number |
|-----------------------|-----------------------------|
| $SW_1 - 8$ | BSS806NH6327XTSA1 |
| $SW_EN1 - 4$ | DMN6075S-7 |
| $Co1 - 4; Cf1 - 3$ | 10uF Kemet Konnet |
| L_{buck} | Würth Elektronik 68 μ H |
| Buck converter | TI LMR16006 |
| Gate driver | Skywork SI8275; TI LM5114 |
| LDO | TI TPS70950 |
| Isolated Power Supply | Murata CRES0505SC |

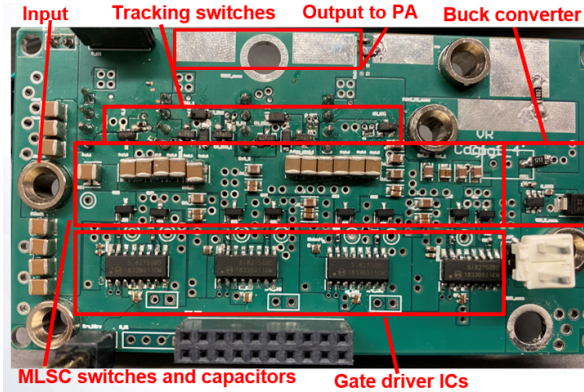


Fig. 4: The AMH Converter prototype

III. IMPLEMENTATION

A prototype of the AMH converter, shown in Figure 4, was implemented using the key components in Table I. The prototype included all power switches, tracker switches, and gate driver circuitry. The converter utilizes dual-channel isolated gate drivers for switches control signals and a cascaded bootstrap and LDOs structure similar to the ones used in [11] to provide proper supplies for the gate drivers of the switches, $SW_1 - 8$. For simplicity in implementation, the PPP Buck converter stage is implemented using the TI LMR16006 product [12].

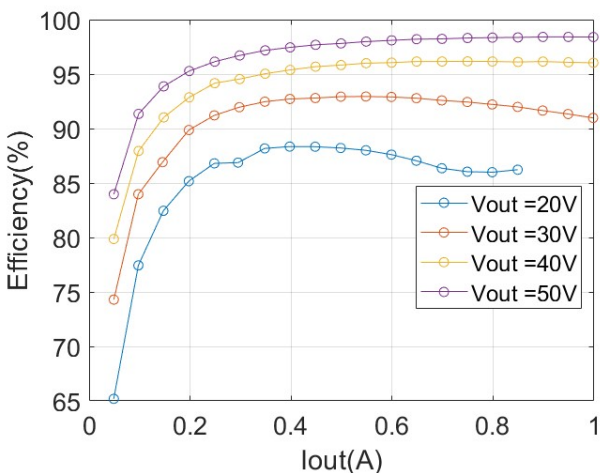


Fig. 5: Efficiency of the AMH converter with $V_{IN} = 50V$ and V_{O0} is regulated at 10V

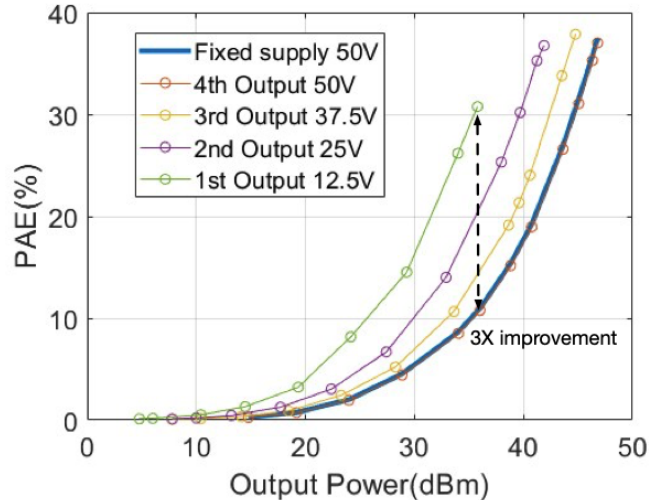


Fig. 6: Efficiency at 4 levels with class-AB PA

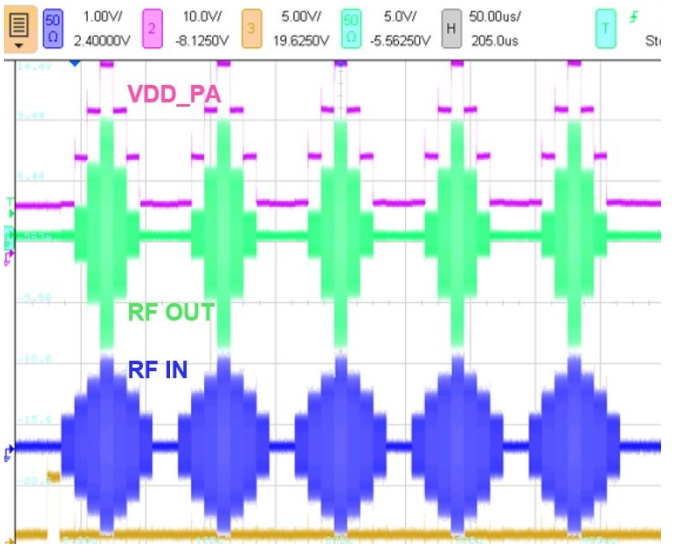


Fig. 7: Symbol Power Tracking with Step CW

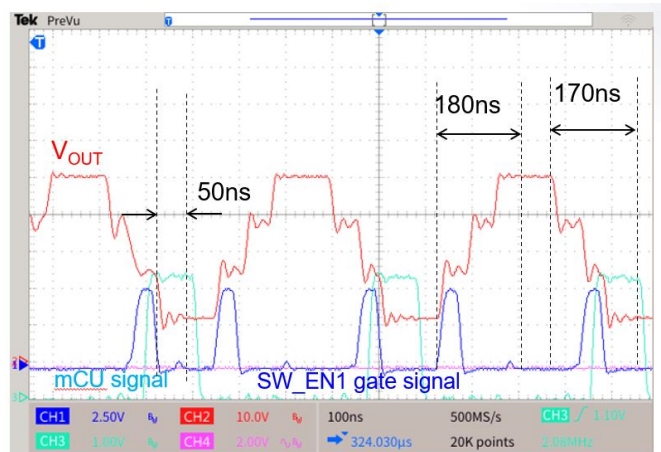


Fig. 8: Voltage level transitions

IV. MEASUREMENT RESULTS

The converter performance is demonstrated in both DC operation and SPT operation. Figure 5 shows the converter DC efficiency when V_{OUT} is connected to one of the four levels while the PPP Buck converter stage regulates V_{O0} at 10V. The converter maintains an efficiency higher than 85% for more than 80% of the load range across all four output levels. The converter efficiency is also measured with a commercial class-AB GaN power amplifier module in Figure 6. Compared with a fixed 50V supply, the power-added efficiency (PAE) can be improved by $\sim 3X$ (from 10% to 30%) at 11dB backoff from the peak power. The symbol tracking operation of the converter is verified in Figure 7. The power of the continuous wave (CW) signal is changed by an example symbol period of $10\mu s$. The corresponding voltage transitions can be predetermined from the input RF signal and synchronized with the output signal as described in Fig. 2. The transition time is $\sim 50\text{ns}$, which is shown in Fig. 8. The fast-level transition time is well within the required cyclic prefix time of 290ns in 5G NR.

V. CONCLUSIONS

In this paper, we have demonstrated a new adjustable multilevel hybrid (AMH) converter architecture that supports a wide output voltage range up to 50V, multiple voltage levels, and a fast voltage level transition of 50ns for symbol power tracking in 5G NR base stations. The converter PCB prototype exhibits an efficiency higher than 85% for a wide range of RF loads and delivers 50W maximum output power with 98.4% efficiency. The converter is proven capable of improving 3X of power-added efficiency at 11 dB backoff power when tested with a commercial class-AB PA.

ACKNOWLEDGMENT

This work was supported in part by the Center for Wireless Communications (CWC) (cwc.ucsd.edu) at UC San Diego, Qorvo, and the NSF CAREER Award No. 2042525.

REFERENCES

- [1] P. Asbeck and Z. Popovic, "Et Comes of Age: Envelope Tracking for Higher-Efficiency Power Amplifiers," *IEEE Microwave Magazine*, vol. 17, no. 3, pp. 16–25, 2016.
- [2] M. C. W. Hoyerby and M. A. E. Andersen, "Ultrafast Tracking Power Supply With Fourth-Order Output Filter and Fixed-Frequency Hysteretic Control," *IEEE Transactions on Power Electronics*, vol. 23, no. 5, pp. 2387–2398, 2008.
- [3] V. Pinon, F. Hasbani, A. Giry, D. Pache, and C. Garnier, "A Single-Chip WCDMA Envelope Reconstruction LDMOS PA with 130MHz Switched-Mode Power Supply," in *2008 IEEE International Solid-State Circuits Conference - Digest of Technical Papers*, 2008, pp. 564–636.
- [4] D. F. Kimball, H. Kazeimi, J. J. Yan, P. T. Theilmann, I. Telleiz, and G. Collins, "Envelope Modulator & X-Band MMICs on Highly Integrated 3D Tunable Microcoax Substrate," in *2015 IEEE Compound Semiconductor Integrated Circuit Symposium (CSICS)*, 2015, pp. 1–4.
- [5] J.-S. Bang, D. Kim, J. Lee, S. Jung, Y. Choo, S. Park, Y.-H. Jung, J.-Y. Ko, T. Norniyama, J. Baek, J. Han, S.-H. Lee, I.-H. Kim, J.-S. Paek, J. Lee, and T. B. Cho, "2-Tx Digital Envelope-Tracking Supply Modulator Achieving 200MHz Channel Bandwidth and 93.6% Efficiency for 2G/3G/LTE/NR RF Power Amplifiers," in *2022 IEEE International Solid- State Circuits Conference (ISSCC)*, vol. 65, 2022, pp. 1–3.
- [6] J. Moon, J. Son, J. Kim, I. Kim, S. Jee, Y. Y. Woo, and B. Kim, "Doherty amplifier with envelope tracking for high efficiency," in *2010 IEEE MTT-S International Microwave Symposium*, 2010, pp. 1086–1089.
- [7] V. Yousefzadeh, E. Alarcon, and D. Maksimovic, "Efficiency optimization in linear-assisted switching power converters for envelope tracking in rf power amplifiers," in *2005 IEEE International Symposium on Circuits and Systems (ISCAS)*, 2005, pp. 1302–1305 Vol. 2.
- [8] G. Lasser, M. Duffy, J. Vance, and Z. Popovic, "Discrete-level envelope tracking for broadband noise-like signals," in *2017 IEEE MTT-S International Microwave Symposium (IMS)*, 2017, pp. 1942–1945.
- [9] M. Vasic, O. Garcia, J. A. Oliver, P. Alou, D. Diaz, J. A. Cobos, A. Gimeno, J. M. Pardo, C. Benavente, and F. J. Ortega, "High efficiency power amplifier for high frequency radio transmitters," in *2010 Twenty-Fifth Annual IEEE Applied Power Electronics Conference and Exposition (APEC)*, 2010, pp. 729–736.
- [10] J.-S. Paek, T. Nomiyama, J. Han, I.-H. Kim, Y. Lee, D. Kim, E. Park, S. Lee, J. Lee, T. B. Cho, and I. Kang, "A 90ns/V Fast-Transition Symbol-Power-Tracking Buck Converter for 5G mm-Wave Phased-Array Transceiver," in *2019 IEEE International Solid- State Circuits Conference - (ISSCC)*, 2019, pp. 240–242.
- [11] R. Das and H.-P. Le, "Gate Driver Circuits With Discrete Components For A GaN-based Multi-Level Multi Inductor Hybrid Converter," *IEEE Transactions on Industrial Electronics*, pp. 1–1, 2022.
- [12] *LMR16006 SIMPLE SWITCHER 60V 0.6A Buck Regulators With High Efficiency ECO Mode*, Texas Instruments, 10 2014.